

Investigation of the effects of binary hybrid nanofluids and different arrangements of corrugated tubes on thermal performance

Fatma Oflaz^{1*} 

¹Firat University, Faculty of Technology, Automotive Engineering, Elazığ, Türkiye

Abstract: This research examined the effects of corrugation distance and nanofluid volume concentration on pressure drop, Nusselt number, and thermal performance in a circular tube. Binary nanofluid (MWCNT/Al₂O₃, 60:40) with volume fractions of 0.25%, 0.5%, and 1% was tested in corrugated tubes with distances of 10 mm, 20 mm, and 30 mm under constant heat flux (20 kW/m²) for Reynolds numbers between 10,000 and 40,000. 3D single-phase model was developed using ANSYS 19 with the standard k-ε turbulence model and validated against equations from the literature. Results revealed that heat transfer improved with increasing Reynolds number, primarily due to elevated flow rates and intensified mixing induced by the corrugated surfaces. Compared to smooth tubes, the corrugated tubes exhibited higher Nusselt numbers, signifying better convective heat transfer performance. Nonetheless, this improvement was accompanied by increased friction factors and pressure drops, especially at shorter corrugation distances. Shorter corrugation distances intensified turbulence and mixing, enhancing heat transfer, while longer distances diminished turbulence, lowering the Nusselt number. The highest thermal performance, with a performance evaluation criterion of 1.27, was achieved at a corrugation distance of 10 mm and an MWCNT/Al₂O₃ nanofluid concentration of 1%. For the same nanofluid concentration, the performance evaluation criterion was 1.24 at a corrugation distance of 20 mm and 1.21 at 30 mm, respectively.

Keywords: Binary nanofluid, Corrugated tube, Heat transfer, Performance Evaluation Criteria, Pressure drop

1. Introduction

Corrugation on tube walls enhances heat transfer by inducing turbulence and swirl flows, which increase fluid mixing and improve interaction with the tube surface. The swirling motion helps clean the inner surface, reducing fouling, while the increased surface area allows for more efficient heat exchanger. These combined factors reduce the fouling factor and enhance overall heat transfer efficiency [1]. Additionally, corrugated tubes increase the wetted perimeter without changing the cross-sectional area, which provides more surface area for heat transfer. Corrugated surfaces improve heat transfer by enhancing turbulence and fluid mixing but cause a higher pressure drop due to increased flow resistance. Corrugated tubes are generally utilized in heating and cooling systems, waste heat recovery, and chemical reactors due to their improved heat transfer efficiency [2]. Corrugated tubes have gained significant attention in research due to their simpler manufacturing and assembly process. Their practical advantages

make them a preferred choice for enhancing heat transfer efficiency. Cauwenberge et al. [3] investigated helical heat exchangers using corrugated tubes and found that these tubes experienced a pressure drop 5.6 to 6.7 times higher than that of smooth tubes. They also observed a substantial improvement in heat transfer performance, with increases between 83% and 119%. Andrade et al. [4] examined the characteristics of heat transfer and pressure drop in corrugated tubes. They found that corrugated tubes exhibit a more gradual shift in frictional behavior compared to smooth tubes, demonstrating greater effectiveness in handling transitional flow regimes. Navickaitė et al. [5] studied numerical analyses to evaluate the thermal performance of corrugated tubes subjected to constant power inputs. The results revealed that double-corrugated tubes significantly improve thermal efficiency while maintaining the same pressure drop. The numerical simulations predicted a 400% increase in thermal efficiency, with a volumetric flow rate 4.2 times lower in double-corrugated tubes. Additionally, PEC increased by up to 14% for tubes

*Corresponding author:

Email: fteber@firat.edu.tr

Cite this article as:

Oflaz, F. (2025). Investigation of the effects of binary hybrid nanofluids and different arrangements of corrugated tubes on thermal performance. *European Mechanical Science*, 9(2): 114-124. <https://doi.org/10.26701/ems.1618871>

History dates:

Received: 13.01.2025, Revision Request: 10.03.2025, Last Revision Received: 20.03.2025, Accepted: 27.04.2025



© Author(s) 2025. This work is distributed under <https://creativecommons.org/licenses/by/4.0/>



Nomenclature

D	diameter (mm)
ΔV	differential voltage, v
Q	rate of heat transfer (W)
h	convective heat transfer coefficient (W/m ² K)
q	heat flux (W/m ²)
cp	specific heat (J kg /K)
ΔP	pressure drop [Pa]
T	temperature (K)
U	average velocity (m/s)

Greek symbols

f	friction factor
Re	Reynolds number
Pr	Prandtl number
ϕ	volume concentration, %
μ	dynamic viscosity (kg/ms)

ρ	density (kg/m ³)
k	thermal conductivity (W/mK)
Nu	Nusselt number
\dot{m}	mass flow rate (kg/s)
EG	ethylene glycol
L	length (mm)
e	thick (mm)
MWCNT	multi-walled carbon nanotubes
Al ₂ O ₃	aluminum oxide
η	overall enhancement efficiency
θ	kinematic viscosity (m ² /s)

Subscripts

bf	base fluid
f	fluid
nf	nanofluid
p	nanoparticle

with an ellipse-base and 11% for those with a super ellipse-base. Wongcharee and Eiamsa-ard [6] performed experimental studies to examine the combined impact of using CuO/water nanofluids, twisted tapes, and corrugated tubes with various flow configurations. The results showed that nanofluids in smooth tubes exhibited a heat transfer improvement ranging from 2.64% to 16.9% over water under identical conditions. Additionally, the use of corrugated tubes resulted in a more significant enhancement, with heat transfer increasing by 4.8% to 66.3%. Ekiciler [7] examined the impact of wall corrugation and the use of Zn:Ag/EG-H₂O hybrid nanofluid on heat transfer and flow in a turbulent pipe flow. Different wall corrugation patterns were compared to a smooth pipe, with Reynolds numbers ranging from 13000 to 28000. The results demonstrated that adding wall corrugations significantly enhanced heat transfer and affected flow characteristics. Ajeel et al. [8] examined various corrugated channels using nanofluids in turbulent flow conditions with a constant heat flux. The results revealed that the modified channels substantially improved the heat transfer rate, with the greatest enhancement occurring in a trapezoidal corrugated channel using 2% silica nanofluids. Wang et al. [9–12] developed innovative external helical corrugated tubes to optimize heat transfer, pressure drop, and energy efficiency. The findings indicate that secondary flow plays a key role in reducing the irreversibility of both heat dissipation and viscous dissipation. Compared to transverse corrugated tubes with similar geometric characteristics, the spiral corrugated tubes demonstrated superior overall performance. Studies show that adding nanoparticles to a base fluid to create “nanofluids” can significantly increase the fluid’s thermal conductivity [13]. This improvement makes nanofluids more effective for heat transfer applications, offering potential benefits in systems like industrial cooling and electronics.

MWCNTs are preferred as nanofluids due to their high thermal conductivity, large surface area, and strong mechanical properties, which enhance heat transfer performance. MWCNTs also offer good stability in suspension and have a low density, minimizing pressure drop and improving overall thermal efficiency. These attributes make MWCNT nanofluids ideal for heat exchange and thermal management applications. In their study, Palanisamy et al. [14] explored the heat transfer and pressure drop characteristics of a cone-shaped helically coiled tube heat exchanger utilizing MWCNT/water nanofluid. Results revealed that the Nusselt numbers, representing the heat transfer efficiency, increased by 22%, 41%, and 52% for nanofluids with volume fractions of 0.1%, 0.3%, and 0.5%, respectively, in comparison to water. This improvement was linked to the enhanced thermal conductivity of MWCNT nanofluids and increased turbulence within the fluid. Ibrahim et al. [15] examined the mixed convection heat transfer behavior of hybrid nanofluids, focusing on how varying nanoparticle compositions impact heat transfer across different flow conditions. Their analysis highlighted the influence of distinct nanoparticle combinations on thermal performance in various flow regimes. They created and evaluated three hybrid nanofluids with distinct Al₂O₃ and MWCNT ratios. Of these, the nanofluid containing 60% Al₂O₃ and 40% MWCNT showed the greatest improvement in heat transfer performance, achieving a Nusselt number increase of more than 5% relative to the other formulations. Painuly et al. [16] carried out an experimental investigation to assess the friction factors and convective heat transfer efficiency of a helically corrugated tube equipped with inserts, specifically under laminar flow conditions. The working fluid was water-ethylene glycol mixture with hybrid nanofluids composed of Al₂O₃ and MWCNT. The results showed that increasing the Al₂O₃-MWCNT

concentration in the hybrid nanofluid, along with reducing the helix ratio of the tube inserts, significantly enhanced both the heat transfer rate and the thermal performance factor. The Al_2O_3 -MWCNT hybrid nanofluid demonstrated Nusselt number increases of 42.5%, 49.47%, and 56.2% over the base fluid at volume fractions of 0.1%, 0.5%, and 1%, respectively. Najafabadi et al. [17] examined three-dimensional simulations of steady-state laminar flow within a horizontal pipe, utilizing engine oil as the base fluid mixed with CuO and multi-walled carbon nanotubes nanoparticles. The objective was to evaluate and compare the impact of varying nanoparticle volume concentrations, using CuO and MWCNT in 1:1 and 1:2 ratios, on convective heat transfer performance. The results showed that increasing the nanoparticle concentration led to significant improvements in both the convective heat transfer coefficient and the Nusselt number, with MWCNT contributing more substantially to the enhancements than CuO. Scott et al. [18] conducted research on the preparation of alumina–multiwalled carbon nanotube/water hybrid nanofluid using a two-step method across different volume concentrations. The findings indicated that increasing the volume concentration initially enhanced heat transfer, with a maximum improvement of 49.27% observed at a volume concentration of 0.10%,

compared to the base fluid. However, beyond this point, further increases in concentration resulted in a decline in natural convection heat transfer performance.

Based on the above studies, most research has focused on the effects of nanofluid types and mass/volume fractions on heat transfer. Some studies have investigated the effects of MWCNT, Al_2O_3 nanofluids, and corrugated tubes separately; however, no study has been found that has investigated their combined effect in the same study. Corrugated tubes are known to enhance heat transfer by disrupting the thermal boundary layer, increasing turbulence and improving fluid mixing. For this purpose, this study aims to analyze the combined effects of MWCNT/ Al_2O_3 hybrid nanofluids with two different corrugation spacings and three different volume concentrations on thermal performance.

2. Materials and methods

2.1. Physical model

The study focuses on a numerical analysis of heat transfer and fluid flow within a 3D corrugated tube. The key objective is to investigate how the corrugated

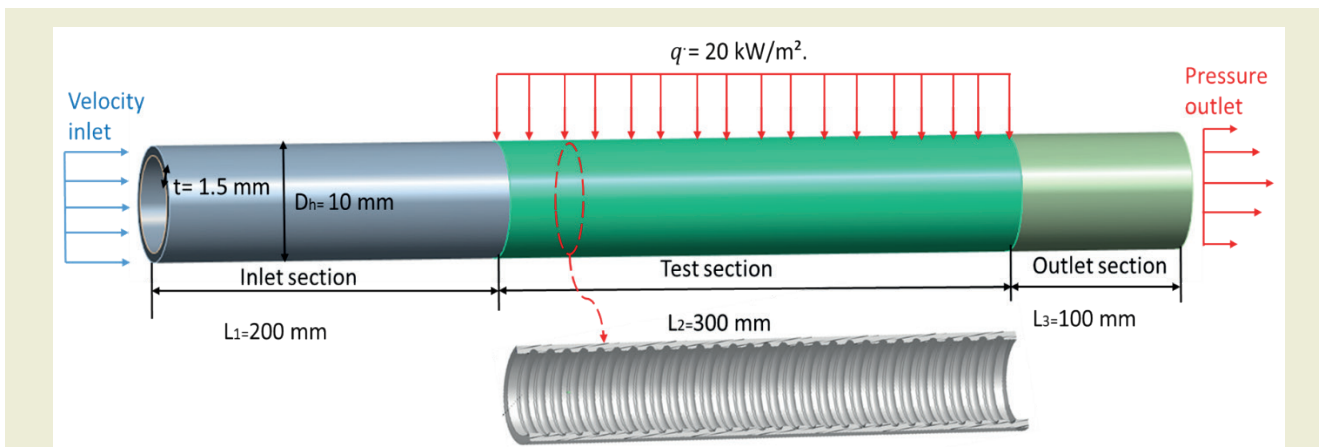


Figure 1. Schematic diagram of corrugated tube

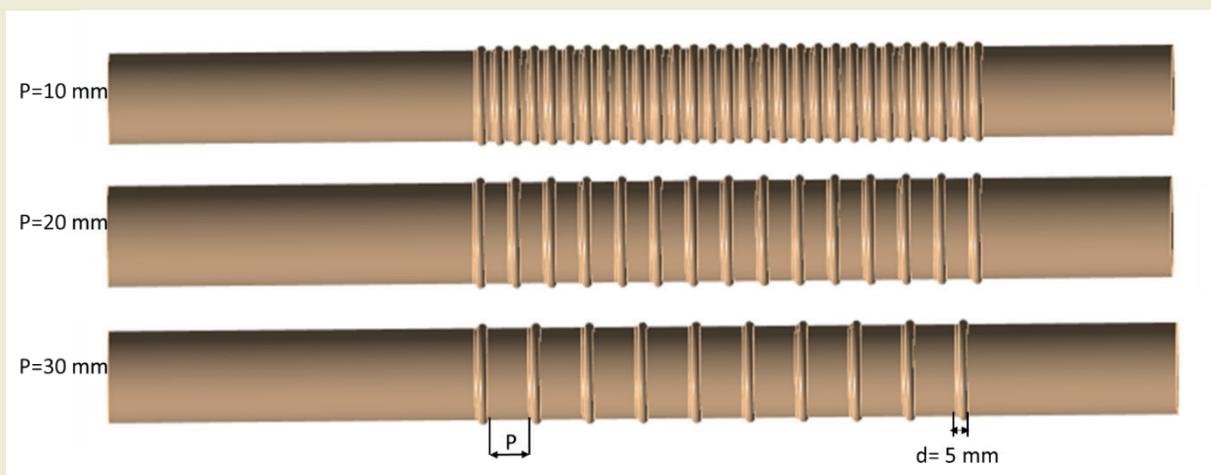


Fig. 2. View of corrugated distances of corrugated tubes

tube's structure affects fluid flow and heat transfer under specified boundary conditions. Two distinct tube geometries were analyzed: a smooth tube and a corrugated tube. The smooth tube served as the baseline for comparison against the performance of the corrugated tube. ► **Figure 1** provides a visual representation of the corrugated tube, illustrating its structure and the associated computational domain. The ► **Figure 1** highlights the corrugated section, as well as the smooth walled inlet and outlet regions that are part of the flow domain used for the analysis. The smooth tube used has the same dimensions as the corrugated tube, except it does not have any corrugations.

The tube is 600 mm long with a 10 mm hydraulic diameter and 1.5 mm wall thickness. It consists of an inlet (200 mm), a heated corrugated test section (300 mm), and an outlet (100 mm). Corrugation spacings are 10 mm, 20 mm, and 30 mm. The inlet ensures fully developed flow (velocity inlet at 300.15 K), while the outlet prevents backflow (pressure outlet). The corrugated walls are heated at 20 kW/m². The flow domain includes smooth inlet/outlet sections and a heated test section for analysis.

2.2. Thermophysical properties of nanofluids

The general equations utilized to determine the thermophysical properties of nanofluids can also be applied to hybrid nanofluids with appropriate modifications. In this context, the base fluid is denoted by (bf), the nanoparticles by (np), and the nanofluid by (nf). Symbols (p₁) and (p₂) specifically refer to MWCNT nanoparticles and Al₂O₃ nanoparticles, respectively.

The volume fraction of the hybrid nanofluid is calculated as follows:

$$\varphi_{hnf} = \varphi_{p1} + \varphi_{p2} \tag{1}$$

The density of the nanofluid is determined using the Pak and Cho [19] correlation, as presented in Equation (2)

$$\rho_{hnf} = \rho_{bf} \cdot (1 - \varphi) + \rho_{np} \cdot \varphi \tag{2}$$

The dynamic viscosity of the hybrid nanofluid is calculated using the well-known Brinkman [20] equation (3), as follows:

$$\mu_{hnf} = \mu_{bf} (1 - \varphi_{p1} - \varphi_{p2})^{-2.5} \tag{3}$$

The thermal conductivity of the hybrid nanofluid was obtained using the commonly used Maxwell [21] equation, as described in equation (4) as follows:

$$k_{hnf} = \frac{(\varphi_{p1} k_{p1} + \varphi_{p2} k_{p2}) / \varphi_{nf} + 2k_{bf} + 2(\varphi_{p1} k_{p1} + \varphi_{p2} k_{p2}) - 2(\varphi_{nf} k_{bf})}{(\varphi_{p1} k_{p1} + \varphi_{p2} k_{p2}) / \varphi_{nf} + 2k_{bf} - 2(\varphi_{p1} k_{p1} + \varphi_{p2} k_{p2}) + \varphi_{nf} k_{bf}} \tag{4}$$

In this study, nanofluids were prepared at three different volume concentrations (0.25%, 0.5% and 1%) using water as the working fluid and MWCNT-Al₂O₃

Table 1. The characteristics of water and the nanoparticles utilized in this study.

Properties	Water [22]	MWCNT [23]	Al ₂ O ₃ [22]
ρ (kg/m ³)	998.2	2100	3980
C_p (J/kg K)	4182	710	777
k (W/mK)	0.6	2000	38

nanoparticles at a ratio of (60:40). A 60:40 hybridization ratio was selected based on the experimental findings of Krishnan et al. [24], which investigated the thermal properties of Al₂O₃-MWCNT/DI water hybrid nanofluids at different particle weight ratios and identified 60:40 as the most thermally efficient composition.

2.3. Data reduction

The findings are evaluated and expressed through the average friction factor (f), Reynolds number (Re), and Nusselt number (Nu), each represented by the following equations:

The constant heat flux applied to the test tube can be expressed as follows:

$$q = \frac{Q}{\pi D_h L} \tag{5}$$

Here, q represents the constant heat flux and D_h is the hydraulic diameter of the tube.

The convective heat transfer coefficient in the tube is described as follows:

$$h = \frac{q}{(T_w - T_b)} \tag{6}$$

Here T_w represents the local wall temperature and T_b represents the temperature of the mass.

$$Re = \frac{\rho U D_h}{\mu} \tag{7}$$

Here U represents the mean fluid velocity.

$$Nu = \frac{h D_h}{k} \tag{8}$$

$$f = \frac{\Delta P}{\frac{1}{2} \rho U^2 \frac{L}{D_h}} \tag{9}$$

The pressure difference (ΔP) is determined by subtracting the average outlet pressure (P_{outlet}) from the average inlet pressure (P_{inlet}), as described in Equation (10).

$$\Delta P = P_{inlet} - P_{outlet} \tag{10}$$

A non-dimensional parameter, PEC is generally defined

as the ratio of increased heat transfer performance to increased friction losses in a heat exchange system. It evaluates whether a particular enhancement technique (e.g. turbulators, vortex generators, nanofluids, extended surfaces) provides an overall benefit in thermal-hydraulic performance. PEC value greater than 1 indicates that the heat transfer improvement outweighs the increase in flow resistance, making the enhancement effective. On the other hand, if PEC is less than 1, the increase in pressure drop is more significant than the thermal gain, rendering the modification inefficient. The Performance Evaluation Criteria, shown in Equation 11, is applied to evaluate the heat transfer efficiency and fluid flow characteristics of tubes with varying surface roughness. It combines the Nusselt number (representing heat transfer) and the friction factor (representing flow resistance) to evaluate overall performance. The PEC assesses whether the increase in heat transfer efficiency is sufficient to offset the additional fluid friction. Here Nu represents corrugated tube and Nu_s represents smooth tube.

$$PEC = \frac{(Nu/Nu_s)}{(f/f_s)^{1/3}} \quad (11)$$

2.4. Governing equations

Finite volume numerical simulations were conducted using ANSYS Fluent 19. To enhance the accuracy in capturing turbulent flows and to improve the modeling of fluid mixing and flow instabilities, the k- ϵ RNG turbulence model was employed under single-phase flow conditions. The pressure and velocity fields were solved iteratively using the SIMPLE algorithm to ensure fluid stability. The QUICK (Quadratic Upstream Interpolation for Convective Kinematics) scheme was employed to enhance accuracy in convective flow calculations, providing smooth flow modeling. The convergence criterion was set to 1×10^{-5} with the relevant equations used generally outlined.

Mass Conservation

$$\nabla(\rho \vec{V}) = 0 \quad (12)$$

Momentum Conservation

$$\nabla(\rho \vec{V} \vec{V}) = -\nabla P + \nabla(\mu \nabla \vec{V}) \quad (13)$$

Energy Conservation

$$\nabla(\rho c_p \vec{V} T) = \nabla(k \nabla T) \quad (14)$$

The k- ϵ turbulence model defines the turbulence kinetic energy (k) and the dissipation rate (ϵ) by solving differential equations that describe the behavior of these turbulent properties.

$$\frac{\partial(\rho k)}{\partial t} + \nabla \cdot (\rho U k) = \nabla \cdot \left(\left(\mu + \frac{\mu_t}{\sigma_k} \right) \nabla k \right) + P_k - \rho \epsilon \quad (15)$$

$$\frac{\partial(\rho \epsilon)}{\partial t} + \nabla \cdot (\rho U \epsilon) = \nabla \cdot \left(\left(\mu + \frac{\mu_t}{\sigma_\epsilon} \right) \nabla \epsilon \right) + \frac{\epsilon}{k} (C_{\epsilon 1} P_k) - C_{\epsilon 2} \rho \epsilon \quad (16)$$

P_k is defined as;

$$P_k = \mu_t \nabla U \cdot (\nabla U + \nabla U^T) - \frac{2}{3} \nabla \cdot U (3\mu_t \nabla \cdot U + \rho k) \quad (17)$$

In this turbulence model, the constant coefficients are as follows: $C_{\mu}=0.09$, $C_{\epsilon 1}=1.44$, $C_{\epsilon 2}=1.92$, $\sigma_k=1$, $\sigma_\epsilon=1.3$

$$\mu_t = \rho c_\mu k^2 / \epsilon \quad (18)$$

2.5. Boundary conditions

This numerical simulation was conducted under the assumptions that the flow is three-dimensional, steady, and fully developed. Natural convection and heat loss to the surroundings were considered negligible, and gravitational effects were ignored. The velocity profile at the inlet was assumed to be smooth, while the thermophysical properties of the hybrid nanofluid were regarded as constant and unaffected by temperature variations. The inlet boundary conditions were set with a defined flow velocity and a temperature of 300.15 K.

Inlet boundary:

$$u = u_{in}, v=w=0, k_{in} = \frac{3}{2} (I u_{in})^2, \epsilon_{in} = C_{\mu}^{3/4} \frac{k^{3/2}}{L_t} \quad (19)$$

Outlet boundary:

The pressure is set to atmospheric pressure, which corresponds to a gauge pressure of zero.

$$\frac{\partial u}{\partial z} = \frac{\partial v}{\partial z} = \frac{\partial w}{\partial z} = 0, \frac{\partial T}{\partial z} = 0, \frac{\partial k}{\partial x} = \frac{\partial \epsilon}{\partial x} = 0 \quad (20)$$

At the wall:

$$u = v = w = 0, q' = q_{wall} \quad (21)$$

2.6. Grid independence and code validation

A steady-state, 3D model was developed to simulate flow dynamics in a corrugated tube. Mesh generation is a critical step in numerical simulations, impacting both accuracy and computational efficiency. Due to the complex flow near the corrugated surface, capturing this region properly is essential for analyzing pressure drop and the Nusselt number. The mesh was created using ANSYS Workbench 19.0 with an unstructured grid, refined near the walls to accurately resolve the laminar viscous sublayer. The y^+ parameter was used to ensure proper mesh quality, especially for turbulent flows, where the boundary layer consists of multiple zones.

- Viscous sublayer ($y^+ < 5$), where viscous forces dominate.
- Buffer layer and log-law region for higher y^+ .

For accurate results, especially when using a turbulence

model like $k-\epsilon$, it's important to keep y^+ less than 5 near the wall to properly resolve the viscous sublayer and avoid errors in predicting flow properties [25].

$$y^+ = \frac{y u_\tau}{\nu} \tag{22}$$

Here, y^+ shows the non-dimensional distance from the wall, where y is the physical distance to the wall, u_τ is the friction velocity, and ν is the kinematic viscosity of the fluid. This study evaluated different mesh structures at Reynolds number of 10000 to ensure that the model provided accurate results. The specific mesh structure with 2.1 million elements was chosen for all analyses because it produced consistent results for the Nusselt number (Nu) and the friction factor (f), with deviations remaining below 2%. This indicates that increasing the mesh density further did not significantly improve the accuracy, making this mesh both efficient and accurate. Additionally, the y^+ value of 2.46 for this mesh indicates that the mesh near the wall was fine enough to accurately capture the flow characteristics, especially within the viscous sublayer, where y^+ values below 5 are recommended. Since this mesh successfully balances accuracy (with minimal deviation in results) and computational cost, it was chosen for further study, as shown in ►Figure 3.

Different mesh sizes were tested to ensure grid independence. The mesh sizes ranged from 0.4 mm to 0.09 mm, and the results for the Nusselt number and friction factor were plotted. Upon comparing the results, it was found that the percentage difference in Nusselt

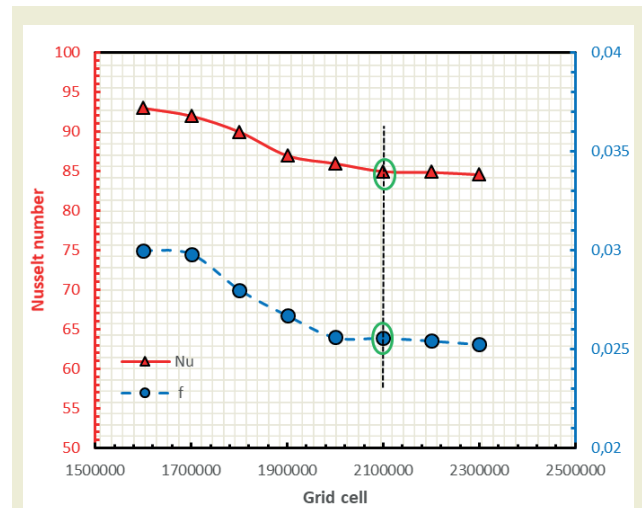


Figure 3. Grid Independence test for Nusselt number and Friction factor at Re=10000

number and friction factor between the finer meshes (0.1 mm, 0.09 mm, and 0.08 mm) was only 1–3%. This small variation indicates that further refining the mesh beyond 0.1 mm would not significantly improve the accuracy of the results but would increase computational cost and time. Thus, the 0.1 mm mesh size was selected as the most appropriate for further analysis. ►Figure 4 illustrates the mesh configuration for the smooth pipe and the corrugated positioned at three different spacing intervals ($P = 10$ mm, $P = 20$ mm, and $P = 30$ mm) using the 0.1 mm mesh structure.

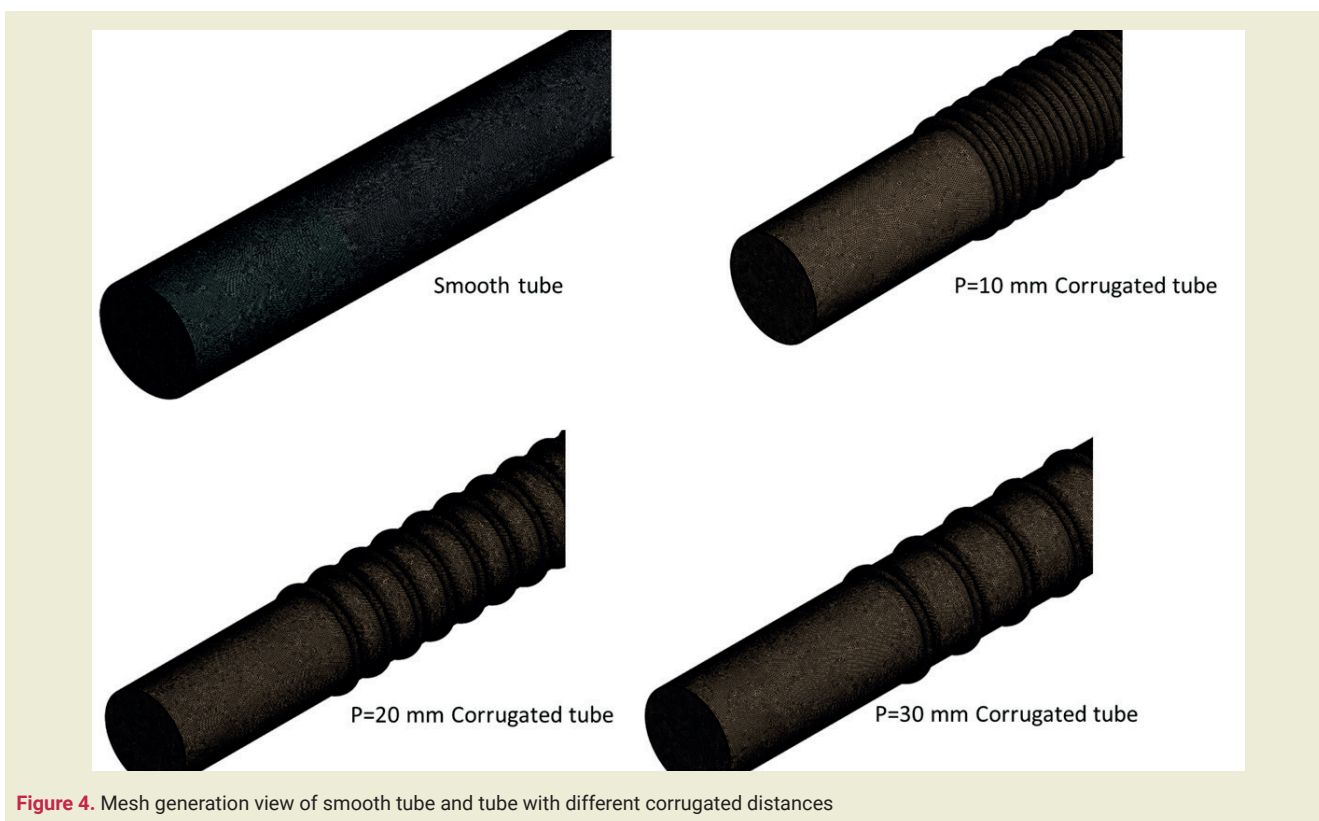


Figure 4. Mesh generation view of smooth tube and tube with different corrugated distances

2.7. Validation of Numerical Study

To ensure the precision and reliability of the numerical method, the results obtained from the simulation of fully developed turbulent water flow in a smooth tube are evaluated against well-known empirical models. The comparisons involved various correlations for the Nusselt number, such as Dittus-Boelter [26] correlation (Equation 23), Gnielinski [27] correlation (Equation 24), and the Pak and Cho [19] correlation (Equation 25), as well as for the friction factor, including Blasius [28] correlation (Equation 26), McAdams [29] correlation (Equation 27), and Petukhov [30] correlation (Equation 28). The CFD simulation results of the Nusselt number and friction factor of the straight pipe were compared with the literature. They were validated against the established literature by showing maximum deviations of $\pm 9\%$ and $\pm 11\%$ respectively, as shown in ► **Figure 4**. This validation confirmed the reliability of the numerical approach in predicting heat transfer and flow resistance under turbulent conditions.

$$Nu = 0.024 Re^{0.8} Pr^{0.4} \quad (23)$$

$$Nu = \frac{(f/8)(Re_D - 1000)Pr}{1 + 12.7(f/8)^{1/2}(Pr^{2/3} - 1)} \quad (24)$$

$$Nu = 0.021 Re_b^{0.8} Pr_{nf}^{0.5}; 10^4 \leq Re_b \leq 10^5 \quad (25)$$

$$f = 0.316 Re^{-0.25} \quad (26)$$

$$f = 0.18 Re^{-2} \quad (27)$$

$$f = (0.29 \ln Re - 1.64)^2 \quad (28)$$

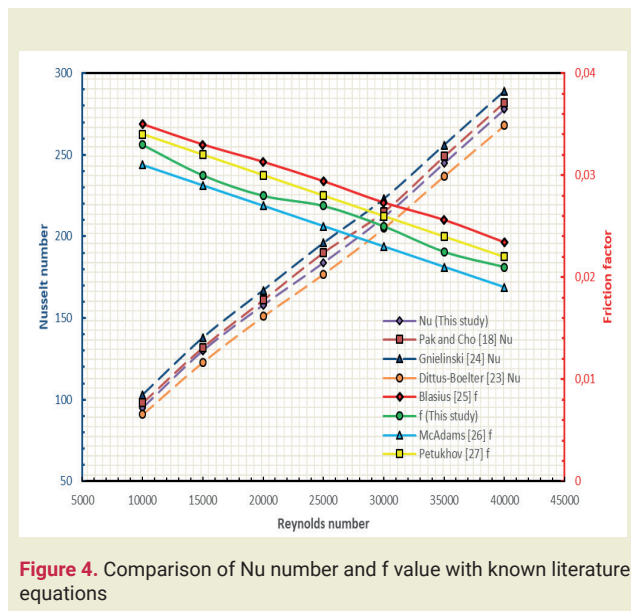


Figure 4. Comparison of Nu number and f value with known literature equations

3. Results and discussion

First, experiments were carried out with water to evaluate the thermal performance of the corrugated pipe without using nanofluid. As shown in ► **Figure 5(a)**, cor-

rugated tubes exhibited higher Nusselt numbers than smooth tubes due to enhanced turbulence, flow separation, and recirculation, which intensified mixing and reduced thermal boundary layer thickness. Heat transfer increased by 37.6%, 32.5%, and 26.3% for corrugation distances of 10 mm, 20 mm, and 30 mm, respectively. ► **Figure 5(b)** shows that the friction factor remained higher in corrugated tubes due to continuous boundary layer disruption, leading to periodic flow separation, re-attachment, and increased resistance.

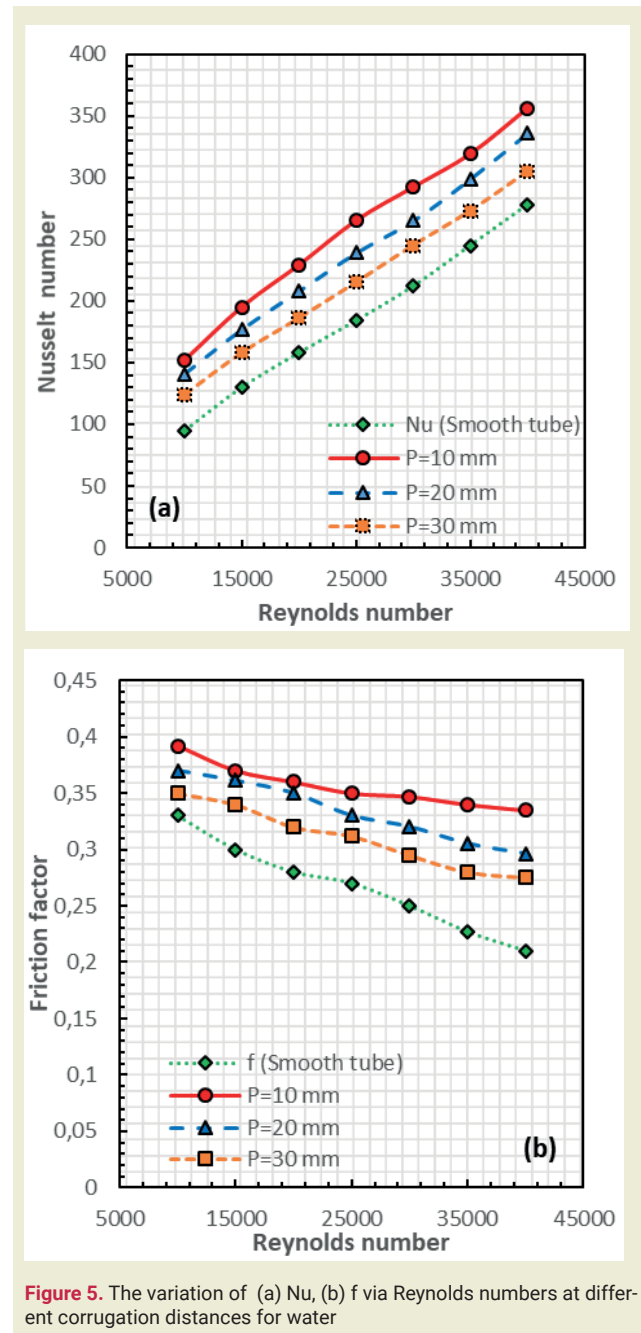


Figure 5. The variation of (a) Nu, (b) f via Reynolds numbers at different corrugation distances for water

The intensified mixing in corrugated tubes enhances heat transfer by transporting cooler fluid from the core to the heated wall and rapidly removing heated fluid. This process reduces the thermal boundary layer thickness, minimizing heat transfer resistance and increasing convective efficiency. As a result, at the same Reyn-

olds number, corrugated tubes achieved higher Nusselt numbers than smooth tubes, with enhancements of 37.6%, 32.5%, and 26.3% for corrugation distances of 10 mm, 20 mm, and 30 mm, respectively. The increased friction factor in corrugated tubes, shown in ►Figure 5(b), is attributed to boundary layer disruption caused by surface geometry. Unlike smooth tubes, where the friction factor decreases with the Reynolds number due to a thinning viscous sublayer, corrugated tubes experience persistent turbulence, flow separation, and recirculation. The repeated formation of low-pressure zones and reattachment points along the corrugated surface further amplifies flow resistance [31].

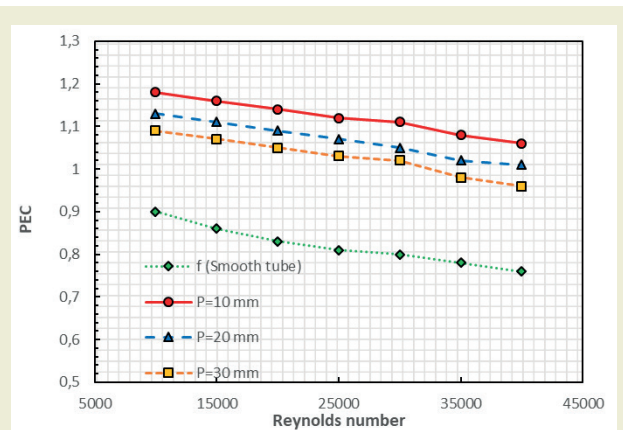


Figure 6. Variation of PEC at different corrugate distances for water

The friction factor in the tube with a corrugate distance of $P = 10$ mm was found to be 15.81 times higher than in the smooth tube. As the distance (P) increases, the interruptions become less frequent, which slightly reduces the friction factor, as seen with $P = 20$ mm and $P = 30$ mm. This shows how strongly the corrugate distance influences flow resistance. However, the friction factor remains significantly higher than that of smooth tubes because each corrugate still induces flow separation and turbulence. Therefore, as the corrugate distance decreases, the flow encounters greater resistance, which is reflected in increasing friction factor values. ►Figure 6 illustrates the PEC for various Reynolds numbers across corrugate distances. Each corrugate distance follows a similar pattern within the Reynolds number range, with PEC values decreasing consistently as Reynolds numbers increase. Among the tested corrugate distances, $P=10$ mm achieves the highest PEC value at 1.18, while $P=30$ mm yields the lowest at 1.09. This suggests closer corrugate distances provide better hydrodynamic performance, whereas higher Reynolds numbers correspond to lower PEC values. These findings emphasize the significant role that corrugate distances play in enhancing flow performance, underscoring the importance of selecting optimal corrugate distance to improve flow efficiency in corrugated tubes.

After analyses conducted on corrugated tubes using water as the working fluid, the thermohydraulic per-

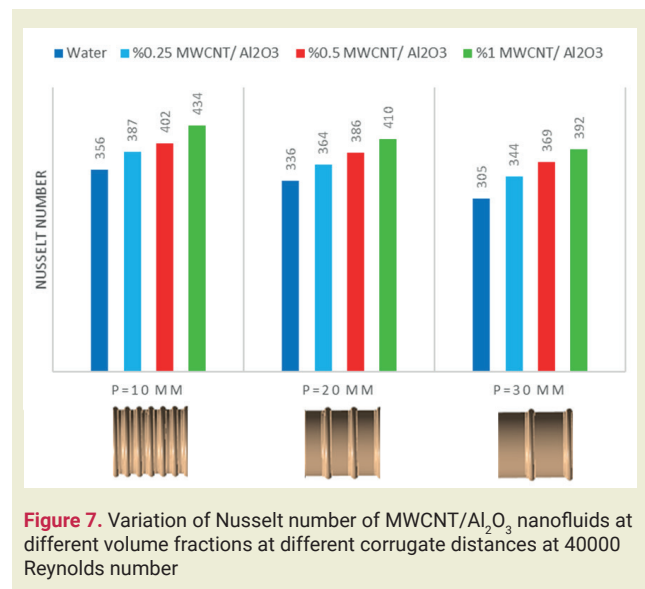


Figure 7. Variation of Nusselt number of MWCNT/Al₂O₃ nanofluids at different volume fractions at different corrugate distances at 40000 Reynolds number

formance of MWCNT/Al₂O₃ nanofluids mixed in a %60-40 ratio was examined at three different volume fractions (0.25%, 0.5%, and 1%). As shown in ►Figure 7, the highest Nusselt number was obtained with the nanofluid containing a 1% volume fraction with a $P=10$ mm pitch. In the corrugated tube with a $P=10$ mm pitch, the 1% MWCNT/Al₂O₃ nanofluid recorded a 17.97% increase in the Nusselt number compared to water. Relative to a smooth, non-corrugated tube, this increase was 35.94%. It was observed that reducing the pitch of the corrugations was more effective than increasing the nanofluid volume fraction. This can be attributed to the fact that refining the physical design of the tube (such as by reducing the corrugate distance) enables efficient enhancement of both convective and conductive heat transfer processes with minimal extra energy input. In contrast, higher nanoparticle concentrations often yield diminishing returns, as they increase the fluid's viscosity and the associated pumping energy needed to maintain flow.

►Figure 8 shows the change in the friction factor of MWCNT/Al₂O₃ nanofluid and water at different volume fractions as the corrugate distance increases with a Reynolds number of 10000. The friction factor decreases with increasing corrugate distance but increases as the nanofluid volume fraction increases. The highest friction factor was obtained in the corrugated tube with a 1% MWCNT/Al₂O₃ volume fraction and a corrugate distance of $P=10$ mm. Compared to the case using water, it was observed that using a 1% MWCNT/Al₂O₃ nanofluid increased the friction factor by 11.51%. This indicates that the use of corrugates causes more friction increase than the use of nanofluids.

►Figure 9 shows the performance of MWCNT/Al₂O₃ nanofluids with three different volume concentrations at three different corrugate distances. The highest performance evaluation criterion was obtained with the

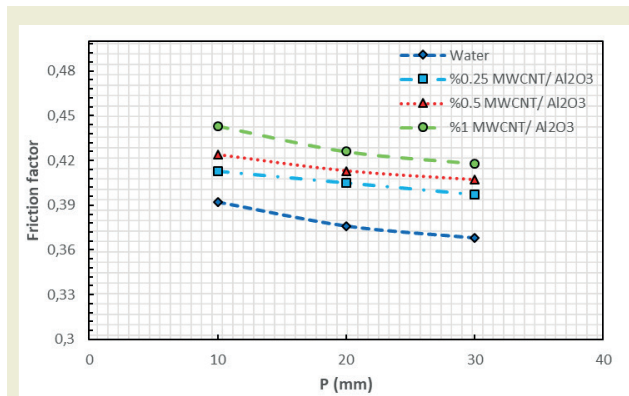


Figure 8. Effect of the corrugate distance on the friction factor of MWCNT/Al₂O₃ nanofluid and water at different volume fractions at 10000 Reynolds number

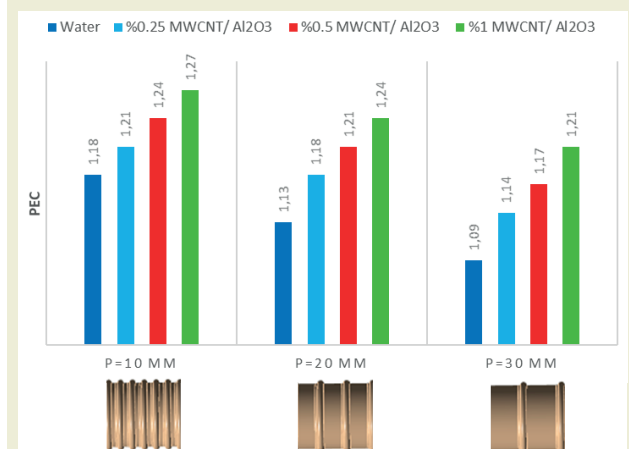


Figure 9. Change in performance evaluation criteria (PEC) of MWCNT/Al₂O₃ nanofluid with different volume fraction at different corrugate distances at 10000 Reynolds number

MWCNT/Al₂O₃ nanofluid with 1% volume concentration at $P = 10$ mm groove distance with a value of 1.27. The lowest value was obtained with the MWCNT/Al₂O₃ nanofluid with 0.25% volume concentration at $P = 30$ mm groove distance with a value of 1.14.

Finally, a comparison was made with experimental studies in the literature to evaluate the performance of this study. As seen in **Figure 10**, the thermal performance of studies conducted using different corrugated tubes was assessed. Qi et al. [32] examined flow resistance and heat transfer performance of TiO₂-water nanofluids in corrugated and circular tubes using experimental and numerical methods. The results showed that adding nanoparticles did not significantly increase the resistance, but the corrugated tube combined with nanofluids increased the heat transfer by up to 53.95%. Hu et al. [33] studied the effects of corrugated tubes parameters on thermal-hydraulic performance using three different corrugated tubes and air and helium as working fluids. It was observed that the Nusselt number (Nu) increased with decreasing p/d ratio. The best-performing corrugated tube exhibited a 60% higher Nu value compared to the smooth tube. Additionally, the

maximum PEC value was recorded at approximately 1.09.

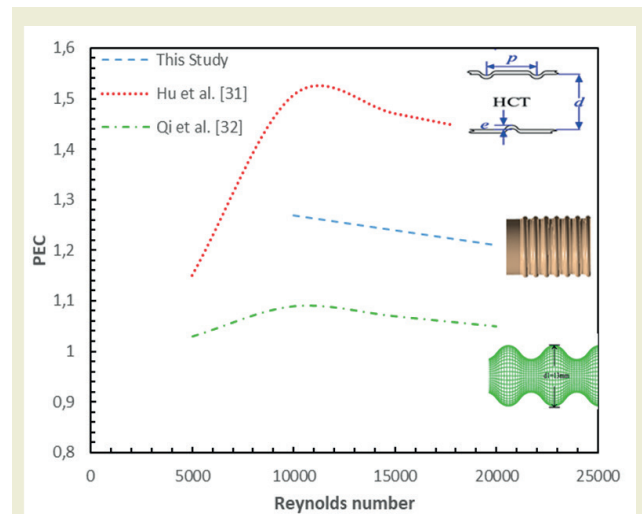


Figure 10. Comparison with literature studies using corrugated tube

4. Conclusions

This study investigated the effects of corrugation distance on the performance of MWCNT/Al₂O₃ nanofluid with different volume concentrations in corrugated tubes. For corrugations with distances of $P=10$ mm, $P=20$ mm, and $P=30$ mm, MWCNT/Al₂O₃ nanofluids mixed at a 60:40 ratio were analyzed at volume fractions of 0.25%, 0.5%, and 1% using the ANSYS Workbench 19.0 program. The Reynolds numbers ranged from 10000 to 40000. This analysis aimed to examine the interaction between heat transfer, friction factor, and pressure drop, providing important insights for improving and optimizing such systems. The main conclusions derived from this study are as follows:

- Corrugated tubes demonstrated superior Nusselt numbers compared to smooth tubes, attributed to enhanced recirculation, backflow, and the formation of a thinner boundary layer. The Nusselt number in corrugated tubes increased significantly compared to the smooth tube, with enhancements of 37.6% for a corrugation distance of 10 mm, 32.5% for 20 mm, and 26.3% for 30 mm.
- Corrugated surfaces increase friction factors compared to smooth tubes. The corrugated surfaces disrupt the normally smooth viscous sublayer, causing greater interaction between the flow and the tube walls, which increases flow resistance and friction. The tube with a corrugation distance of 10 mm exhibited a friction factor 15.81 times higher than that of the smooth tube. Increasing the corrugation distance to 20 mm and 30 mm reduced the frequency of flow disruptions, leading to a slight decrease in the friction factor.

- Reducing corrugate distance increases turbulence and fluid mixing, leading to higher Nusselt numbers, indicating improved heat transfer. In contrast, increasing corrugate distance produces less turbulence and mixing, resulting in lower Nusselt numbers and reduced heat transfer efficiency.
- Smaller corrugate distances improve hydrodynamic performance. However, as the Reynolds number increases, the performance evaluation criteria (PEC) values decrease for all corrugate distances. The maximum performance evaluation criterion of 1.27 was achieved using the MWCNT/Al₂O₃ nanofluid with a 1% volume concentration at a groove distance of 10 mm.
- Increasing the volume fraction of a nanofluid enhances heat transfer through better thermal conductivity, while changes in corrugation distance have a more significant impact on heat transfer by altering the flow structure, increasing turbulence, and strengthening convection.
- This study evaluated the thermal performance of MWCNT/Al₂O₃ hybrid nanofluids at concentrations of 0.25%, 0.50%, and 1%, with the most effective heat transfer observed at 1%. Although increasing the concentration beyond this value may further enhance thermal conductivity, it could also result in undesirable effects such as higher viscosity, increased energy consumption for fluid circulation, and nanoparticle clustering, which may deteriorate flow stability and overall system efficiency.

Future studies could explore the existence of an optimal concentration (peak point) by examining a wider range of concentrations and evaluating the trade-offs between thermal performance and fluid flow characteristics.

Research ethics

Not applicable.

Author contributions

The author solely conducted all stages of this research.

Competing interests

The author state(s) no conflict of interest.

Research funding

None declared.

Data availability

Not applicable.

Peer-review

Externally peer-reviewed.

Orcid

Fatma Oflaz  <https://orcid.org/0000-0002-9636-5746>

References

- [1] Kalendar, A., Galal, T., Al-Saftawi, A. and Zedan, M. (2011) Enhanced tubing thermal performance for innovative MSF system. *Journal of Mechanical Science and Technology*, 25, 1969–77. <https://doi.org/10.1007/s12206-011-0524-7>
- [2] Kareem, Z.S., Mohd Jaafar, M.N., Lazim, T.M., Abdullah, S. and Abdulwahid, A.F. (2015) Passive heat transfer enhancement review in corrugation. *Experimental Thermal and Fluid Science*, Elsevier Inc. 68, 22–38. <https://doi.org/10.1016/j.exptthermflusci.2015.04.012>
- [3] Van Cauwenberge, D.J., Dedeyne, J.N., Van Geem, K.M., Marin, G.B. and Floré, J. (2018) Numerical and experimental evaluation of heat transfer in helically corrugated tubes. *AIChE Journal*, 64, 1702–13. <https://doi.org/10.1002/aic.16038>
- [4] Andrade, F., Moita, A.S., Nikulin, A., Moreira, A.L.N. and Santos, H. (2019) Experimental investigation on heat transfer and pressure drop of internal flow in corrugated tubes. *International Journal of Heat and Mass Transfer*, Elsevier Ltd. 140, 940–55. <https://doi.org/10.1016/j.ijheatmasstransfer.2019.06.025>
- [5] Navickaitė, K., Cattani, L., Bahl, C.R.H. and Engelbrecht, K. (2019) Elliptical double corrugated tubes for enhanced heat transfer. *International Journal of Heat and Mass Transfer*, 128, 363–77. <https://doi.org/10.1016/j.ijheatmasstransfer.2018.09.003>
- [6] Wang, G., Qi, C., Liu, M., Li, C., Yan, Y. and Liang, L. (2019) Effect of corrugation pitch on thermo-hydraulic performance of nanofluids in corrugated tubes of heat exchanger system based on exergy efficiency. *Energy Conversion and Management*, 186, 51–65. <https://doi.org/10.1016/j.enconman.2019.02.046>
- [7] Ekciler, R. (2024) Analysis and Evaluation of the Effects of Uniform and Non-uniform Wall Corrugation in a Pipe Filled with Ternary Hybrid Nanofluid. *Arabian Journal for Science and Engineering*, Springer Berlin Heidelberg. 49, 2681–94. <https://doi.org/10.1007/s13369-023-08459-4>
- [8] Ajeel, R.K., Saiful-Islam, W., Sopian, K. and Yusoff, M.Z. (2020) Analysis of thermal-hydraulic performance and flow structures of nanofluids across various corrugated channels: An experimental and numerical study. *Thermal Science and Engineering Progress*, 19. <https://doi.org/10.1016/j.tsep.2020.100604>
- [9] Wang, W., Zhang, Y., Lee, K.S. and Li, B. (2019) Optimal design of a double pipe heat exchanger based on the outward helically corrugated tube. *International Journal of Heat and Mass Transfer*, Elsevier Ltd. 135, 706–16. <https://doi.org/10.1016/j.ijheatmasstransfer.2019.01.115>
- [10] Wang, W., Zhang, Y., Li, B. and Li, Y. (2018) Numerical investigation of tube-side fully developed turbulent flow and heat transfer in outward corrugated tubes. *International Journal of Heat and Mass Transfer*, Elsevier Ltd. 116, 115–26. <https://doi.org/10.1016/j.ijheatmasstransfer.2017.09.003>
- [11] Wang, W., Zhang, Y., Liu, J., Li, B. and Sundén, B. (2018) Numerical investigation of entropy generation of turbulent flow in a novel outward corrugated tube. *International Journal of Heat and Mass Transfer*, Elsevier Ltd. 126, 836–47. <https://doi.org/10.1016/j.ijheatmasstransfer.2018.06.017>
- [12] Wang, W., Zhang, Y., Li, Y., Han, H. and Li, B. (2018) Multi-objective

- optimization of turbulent heat transfer flow in novel outward helically corrugated tubes. *Applied Thermal Engineering*, Elsevier Ltd. 138, 795–806. <https://doi.org/10.1016/j.applthermaleng.2017.12.080>
- [13] Ofiaz, F., Keklikcioglu, O. and Ozceyhan, V. (2022) Investigating thermal performance of combined use of SiO₂-water nanofluid and newly designed conical wire inserts. *Case Studies in Thermal Engineering*, Elsevier Ltd. 38, 102378. <https://doi.org/10.1016/j.csite.2022.102378>
- [14] Palanisamy, K. and Kumar, P.C.M. (2017) Heat transfer enhancement and pressure drop analysis of a cone helical coiled tube heat exchanger using MWCNT/water nanofluid. *Journal of Applied Fluid Mechanics*, 10, 7–13. <https://doi.org/10.36884/jafm.10.SI.28265>
- [15] Umar Ibrahim, I., Sharifpur, M. and Meyer, J.P. (2024) Mixed Convection Heat Transfer Characteristics of Al₂O₃ – MWCNT Hybrid Nanofluid under Thermally Developing Flow; Effects of Particles Percentage Weight Composition. *Applied Thermal Engineering*, Elsevier Ltd. 249, 123372. <https://doi.org/10.1016/j.applthermaleng.2024.123372>
- [16] Painuly, A., Joshi, G., Negi, P., Zainith, P. and Mishra, N.K. (2025) Experimental analysis of W/EG based Al₂O₃-MWCNT non-Newtonian hybrid nanofluid by employing helical tape inserts inside a corrugated tube. *International Journal of Thermal Sciences*, Elsevier Masson SAS. 208, 109399. <https://doi.org/10.1016/j.ijthermalsci.2024.109399>
- [17] Khalili Najafabadi, M., Hriczó, K. and Bognár, G. (2024) Enhancing the heat transfer in CuO-MWCNT oil hybrid nanofluid flow in a pipe. *Results in Physics*, 64. <https://doi.org/10.1016/j.rinp.2024.107934>
- [18] Scott, T.O., Ewim, D.R.E. and Eloka-Eboka, A.C. (2023) Experimental study on the influence of volume concentration on natural convection heat transfer with Al₂O₃-MWCNT/water hybrid nanofluids. *Materials Today: Proceedings*, Elsevier Ltd. c, 0–6. <https://doi.org/10.1016/j.matpr.2023.07.290>
- [19] Pak, B.C. and Cho, Y.I. (1998) Hydrodynamic and heat transfer study of dispersed fluids with submicron metallic oxide particles. *Experimental Heat Transfer*, 11, 151–70. <https://doi.org/10.1080/08916159808946559>
- [20] H.C., B. (1952) The viscosity of concentrated suspensions and solutions. *J Chem Phys* 20 571.
- [21] Xu, J.Z., Gao, B.Z. and Kang, F.Y. (2016) A reconstruction of Maxwell model for effective thermal conductivity of composite materials. *Applied Thermal Engineering*, 102, 972–9. <https://doi.org/10.1016/j.applthermaleng.2016.03.155>
- [22] Ofiaz, F. (2025) Evaluation of the thermo - hydraulic behavior of water - based graphene and Al₂O₃ hybrid nanofluids in a circular tube through CFD simulations. *Journal of Thermal Analysis and Calorimetry*, Springer International Publishing. <https://doi.org/10.1007/s10973-025-13993-4>
- [23] Keklikcioglu, O. (2023) Optimization of thermal and hydraulic characteristics of a heat exchanger tube using ternary hybrid nanofluids with various configurations. *Journal of Thermal Analysis and Calorimetry*, Springer International Publishing. 148, 7855–67. <https://doi.org/10.1007/s10973-023-12263-5>
- [24] Suseel Jai Krishnan, S., Momin, M., Nwaokocho, C., Sharifpur, M. and Meyer, J.P. (2022) An empirical study on the persuasive particle size effects over the multi-physical properties of monophasic MWCNT-Al₂O₃ hybridized nanofluids. *Journal of Molecular Liquids*, Elsevier B.V. 361, 119668. <https://doi.org/10.1016/j.molliq.2022.119668>
- [25] Ao, S.I., Castillo, O., Douglas, C., Dagan Feng, D. and Korsunsky, A.M. (2017) Proceedings of the international multicongress of engineers and computer scientists 2017. *Lecture Notes in Engineering and Computer Science*, 2227.
- [26] F.W. Dittus, L.M.K.B. (1930) Heat transfer in automobile radiators of the tubular type. *The University of California Publications on Engineering*, 2, 443–61.
- [27] Gnielinski, V. (1976) New equations for heat and mass transfer in turbulent pipe and channel flow. *International Chemical Engineering*, 27, 359–368.
- [28] H. Blasius. (1913) The Law of Similarity for Frictions in Liquids, "Notices of research in the field of engineering. *Not Res F Eng*, 131, 1–41.
- [29] McAdams, W.H. (1942) *Heat Transmission*. (Second Ed), McGraw-Hill, New York,.
- [30] B.S. Petukhov. (1970) Heat Transfer and Friction in Turbulent Pipe Flow with Variable Physical Properties. *Advances in Heat Transfer*, 6, 503–64.
- [31] Togun, H., Homod, R.Z., Yaseen, Z.M., Abed, A.M., Dhabab, J.M., Ibrahim, R.K. et al. (2022) Efficient Heat Transfer Augmentation in Channels with Semicircle Ribs and Hybrid Al₂O₃-Cu/Water Nanofluids. *Nanomaterials*, 12. <https://doi.org/10.3390/nano12152720>
- [32] Hu, Q., Qu, X., Peng, W. and Wang, J. (2022) Experimental and numerical investigation of turbulent heat transfer enhancement of an intermediate heat exchanger using corrugated tubes. *International Journal of Heat and Mass Transfer*, Elsevier Ltd. 185, 122385. <https://doi.org/10.1016/j.ijheatmasstransfer.2021.122385>
- [33] Qi, C., Wan, Y.L., Li, C.Y., Han, D.T. and Rao, Z.H. (2017) Experimental and numerical research on the flow and heat transfer characteristics of TiO₂-water nanofluids in a corrugated tube. *International Journal of Heat and Mass Transfer*, Elsevier Ltd. 115, 1072–84. <https://doi.org/10.1016/j.ijheatmasstransfer.2017.08.098>